Bending localization of nitrous oxide under anharmonicity and Fermi coupling: the dynamical potential approach*

Zhang Chi(张 弛)[a], Fang Chao(房 超)[b] and Wu Guo-Zhen(吴国祯)[a]†

[a] *Molecular and Nano Sciences Laboratory, Department of Physics, Tsinghua University, Beijing* 100084, *China*

[b] *Institute of Nuclear and New Energy Technology, Tsinghua University, Beijing* 100084, *China*

(Received 22 March 2010; revised manuscript received 28 May 2010)

This paper studies the vibrational nonlinear dynamics of nitrous oxide with Fermi coupling between the symmetric stretching and bending coordinates by classical dynamical potential approach. This is a global approach in the sense that the overall dynamics is evidenced by the classical nonlinear variables such as the fixed points and the focus are on a set of levels instead of individual ones. The dynamics of nitrous oxide is demonstrated to be not so much dependent on the excitation energy. Moreover, the localized bending mode is shown to be ubiquitous in all the energy range studied.

Keywords: nitrous oxide, dynamical potential, Fermi coupling, bending localization

PACC: 0545M, 3115Q

1. Introduction

The vibrational dynamics of nitrous oxide has been studied[1−3] and it was found[3] that as the excitation energy is not too high, the dynamics is dominated by the anharmonicity and Fermi coupling between the symmetric stretching and bending coordinates and is, therefore, integrable[4] with the antisymmetric stretching variables decoupled off.[5] This dynamics has been well known and works[5−7] have been devoted to its analysis based on the spectroscopic Hamiltonian which is a fitted algebraic Hamiltonian with its eigenenergies well correlated to the experimental observations. Parallelly, we have recently deviced an algorithm which also starts from the spectroscopic Hamiltonian. However, we note that by transforming it into the coset space (physically this is equivalent to the Heisenberg correspondence), a so-called dynamical potential[8−11] can be readily constructed thereby the global dynamics becomes very obvious visually. In fact, the dynamical potential is characterized by the classical fixed points. Essentially, this approach is closely related to the the bifurcation/fixed point analysis in the nonlinear dynamics.[12] However, it is more of a friendly user. By this approach, the so-called action populations, action percentages and action integrals can be easily defined and calculated so that much of the system dynamics can be unfolded which in certain cases can be comparable to the semiclassical wave function treatment.[13,14] The intention of this work is to apply this approach to nitrous oxide to reveal its vibrational dynamical properties. We will find that this dynamics is not so much dependent on the excitation energy in the energy range studied. Moreover, the localized bending mode is shown to be ubiquitous in all the energy range studied. The localization appears to be prevalent as we have encountered in the cases of HCP, DCP, HOCl and HOBr.[13,14]

In the following, the coset-represented Hamiltonian will be first introduced. Then, the analysis based on the dynamical potentials, fixed points, action populations, action percentages and action integrals will be followed. Finally, a concluding remark will be addressed.

2. The coset space represented Hamiltonian

The algebraic Hamiltonians of nitrous oxide including their coefficients have been determined in Ref. [3]. As pointed out above, when the excitation

*Project supported by the Research Foundation from Ministry of Education of China (Grant No 306020), the Specialized Research Fund for the Doctoral Program of Higher Education, China (Grant No 20060003050), and the National Natural Science Foundation of China (Grant No 20773073).

†Corresponding author. E-mail: wgz-dmp@tsinghua.edu.cn

© 2010 Chinese Physics Society and IOP Publishing Ltd

Table 1. The coefficients for the algebraic Hamiltonian.

parameter /cm^{-1}		parameter /cm^{-1}	
ω_1	1298.59011	y_{112}	−0.116084
ω_2	596.2937	y_{113}	−0.34311
ω_3	2281.99814	y_{122}	−0.035329
x_{11}	−3.9178	y_{123}	0.51513
x_{12}	−3.0087	y_{133}	0.05979
x_{13}	−27.20721	y_{222}	−0.0131887
x_{22}	0.5432	y_{223}	0.046411
x_{23}	−14.58513	y_{233}	0.009261
x_{33}	−15.16516	y_{333}	0.015737
y_{111}	−0.004714	$F_e^{(2)}$	−17.963240

in not high enough, the dynamics is mainly governed by the anharmonicity and Fermi coupling between the symmetric stretching and bending coordinates. Therefore, a simplified Hamiltonian will be adopted as shown below to serve our purpose. For notation, the subscripts, 1, 2 and 3 are used for symmetric stretch, N–N–O bend and antisymmetric stretch respectively. n, ω, x, y are for the action, linear and nonlinear coefficients respectively, $F_{\rm e}^{(2)}$ is for the Fermi coupling, a^+ and a are the creation and destruction operators respectively. For reference, they are summarized in Table 1.

The algebraic Hamiltonian is of the form :

$$
\begin{aligned}
H =& H_0 + H_0^{\rm anh} + H_1,\\
H_0 =& \omega_1\Big(n_1+\frac{1}{2}\Big) + \omega_2(n_2+1) + \omega_3\Big(n_3+\frac{1}{2}\Big),\\
H_0^{\rm anh} =& x_{11}\Big(n_1+\frac{1}{2}\Big)^2 + x_{12}\Big(n_1+\frac{1}{2}\Big)(n_2+1) + x_{13}\Big(n_1+\frac{1}{2}\Big)\Big(n_3+\frac{1}{2}\Big)\\
&+ x_{22}(n_2+1)^2 + x_{23}(n_2+1)\Big(n_3+\frac{1}{2}\Big) + x_{33}\Big(n_3+\frac{1}{2}\Big)^2\\
&+ y_{111}\Big(n_1+\frac{1}{2}\Big)^3 + y_{112}\Big(n_1+\frac{1}{2}\Big)^2(n_2+1) + y_{113}\Big(n_1+\frac{1}{2}\Big)^2\Big(n_3+\frac{1}{2}\Big)\\
&+ y_{122}\Big(n_1+\frac{1}{2}\Big)(n_2+1)^2 + y_{123}\Big(n_1+\frac{1}{2}\Big)(n_2+1)\Big(n_3+\frac{1}{2}\Big) + y_{133}\Big(n_1+\frac{1}{2}\Big)\Big(n_3+\frac{1}{2}\Big)^2\\
&+ y_{222}(n_2+1)^3 + y_{223}(n_2+1)^2\Big(n_3+\frac{1}{2}\Big) + y_{233}(n_2+1)\Big(n_3+\frac{1}{2}\Big)^2 + y_{333}\Big(n_3+\frac{1}{2}\Big)^3,\\
H_1 =& F_e^{(2)}(a_1^+ a_2 a_2 + \text{h.c.}).
\end{aligned}
$$

This Hamiltonian is semiclassical in the sense that it is based on the model of coupled Morse oscillators with Fermi coupling between the bending and symmetric stretching coordinates which is described by the second quantization operators. According to Ref. [3], as the excitation is not too high, the antisymmetric stretch is well decoupled from the rest two motions. Hence, n_3 is set to 0 in our treatment. In this way, there is another conserved action, called polyad number,[6] $P = 2n_2 + n_1$. The P will be limited to 22 in our analysis as suggested by Ref. [3]. The quantized energy levels can be obtained by diagonalizing the above algebraic Hamiltonian matrix constructed by the bases $\{|n_1, n_2 = (P-n_1)/2>\}$ for a given P.

For the further semiclassical treatment, Heisengberg correspondence[15] is used to transform the second quantization operators to classical quantities. Mathematically, this is equivalent to transforming to the coset space.[16] The coset space is a phase space for the vibrational dynamics. This transformation is accomplished through the substitution, $n_1 = (q_1^2+p_1^2)/2$, $n_2 = P-(q_1^2+p_1^2)$. The coset space represented Hamiltonians are:

$$
\begin{aligned}
H_0 =& \omega_1\Big(\frac{1}{2}(p_1^2+q_1^2)+\frac{1}{2}\Big) + \omega_2\big(P-(p_1^2+q_1^2)+1\big) + \omega_3\Big(0+\frac{1}{2}\Big),\\
H_0^{\rm anh} =& x_{11}\Big(\frac{1}{2}(p_1^2+q_1^2)+\frac{1}{2}\Big)^2 + x_{12}\Big(\frac{1}{2}(p_1^2+q_1^2)+\frac{1}{2}\Big)\big(P-(p_1^2+q_1^2)+1\big) + x_{13}\Big(\frac{1}{2}(p_1^2+q_1^2)+\frac{1}{2}\Big)\Big(0+\frac{1}{2}\Big)\\
&+ x_{22}\big(P-(p_1^2+q_1^2)+1\big)^2 + x_{23}\big(P-(p_1^2+q_1^2)+1\big)\Big(0+\frac{1}{2}\Big) + x_{33}\Big(0+\frac{1}{2}\Big)^2\\
&+ y_{111}\Big(\frac{1}{2}(p_1^2+q_1^2)+\frac{1}{2}\Big)^3 + y_{112}\Big(\frac{1}{2}(p_1^2+q_1^2)+\frac{1}{2}\Big)^2\big(P-(p_1^2+q_1^2)+1\big)\\
&+ y_{113}\Big(\frac{1}{2}(p_1^2+q_1^2)+\frac{1}{2}\Big)^2\Big(0+\frac{1}{2}\Big) + y_{122}\Big(\frac{1}{2}(p_1^2+q_1^2)+\frac{1}{2}\Big)\big(P-(p_1^2+q_1^2)+1\big)^2
\end{aligned}
$$

$$+ y_{123}\Big(\frac{1}{2}(p_1^2+q_1^2)+\frac{1}{2}\Big)\big(P-(p_1^2+q_1^2)+1\big)\Big(0+\frac{1}{2}\Big)+y_{133}\Big(\frac{1}{2}(p_1^2+q_1^2)+\frac{1}{2}\Big)\Big(0+\frac{1}{2}\Big)^2$$
$$+ y_{222}\big(P-(p_1^2+q_1^2)+1\big)^3+y_{223}\big(P-(p_1^2+q_1^2)+1\big)^2\Big(0+\frac{1}{2}\Big)$$
$$+ y_{233}\big(P-(p_1^2+q_1^2)+1\big)\Big(0+\frac{1}{2}\Big)^2+y_{333}\Big(0+\frac{1}{2}\Big)^3,$$
$$H_1=\sqrt{2}F_{\rm e}^{(2)}q_1(P-(p_1^2+q_1^2)).$$

The corresponding equations of motion are: $\partial H/\partial q_1 = -\mathrm{d}p_1/\mathrm{d}t$, $\partial H/\partial p_1 = \mathrm{d}q_1/\mathrm{d}t$. This furnishes our tools for the dynamical analysis of this highly excited vibrational system.

Similarly, we can have $H(q_2, p_2, P)$ and the corresponding equations of motion. For short, they will not be shown here.

3. The dynamical potentials, fixed points, action populations, action percentages and action integrals

The dynamical potential[8−11] of $H(q_i, p_i, P)$, $(i = 1, 2)$ is the effective environment in which the q_i coordinate experiences for each P. This is achieved by calculating the maximal and minimal energies by varying p_i for each q_i under the condition that n_1 and n_2 are nonnegative. The dynamical potential composed of these maximal and minimal energies as a function of q_i is a closed curve in which the quantized levels are enclosed. The dynamical potential also defines the q_i region for each level it encloses. The points on the dynamical potential correspond to $\partial H/\partial p_i = 0$. Furthermore, the points on the dynamical potential corresponding to $\partial H/\partial q_i = 0$ are the fixed points in the dynamical space. Therefore, at these fixed points, both n_1 and $n_2/2$ are time invariant. So, the fixed points we mean here are those on which the actions are constant in this dynamical system. We will note that the dynamical potential is mainly composed of two portions with the lower one, more or less, like a (deformed) Morse well (or two wells. See later demonstration. The stable fixed point is on the well bottom) and the upper one like an inverse Morse well. Hence, for the upper realm of the dynamical potential, we have to interpret the potential curve in an inverse (upside down) way that its highest point, corresponding to the well bottom of the inverse Morse well, is a stable fixed point, instead.

For each level, in the allowed q_i region, p_i can be known (from eigenenergy $=H(q_i, p_i)$) and so can n_1 and $n_2/2$, as the functions of q_i, n_1 and $n_2/2$ can be interpreted as the action populations in the dynamical coset space for a level. These quantities are the analogues to the wave function density in the quantal treatment. We may further obtain the action percentages for each level by integrating n_1 and $n_2/2$, respectively, through allowed q_i coordinate and setting their values in percentage. (These action percentages are found independent of the coordinate q_1 or q_2 used.)

For each level, we can calculate the trajectories via eigenenergy $= H(q_i, p_i, P)$ in the coset space. The trajectories are closed contours for each level since the system is integrable. Thereby, we can calculate the action integrals

$$1/2\pi \oint p_i \mathrm{d}q_i$$

along the contours in the (q_1, p_1) and (q_2, p_2) spaces. We will see that these action integrals reflect the very essential properties of the levels imbedded in the dynamical potential.

The dynamical potential, fixed point, action population, action percentage and action integral are the tools which we will employ for the dynamical analysis. In our previous works,[13,14] we have seen that by these quantities, immense information of the vibrational dynamics can be obtained which is even comparable to the traditional Schrödinger wave function approach. By this approach, it is seen that the background of the quantal properties is the classical nonlinear variables, whose fixed points are the core.

4. The dynamics

Figure 1 shows the two dynamical potentials in terms of q_1 and q_2 coordinates for $P = 22$, in which there are 12 levels embedded. Levels are labeled by L0, L1,... from the highest one down to the lowest one. It is interesting to note that even for other

smaller polyad numbers, their dynamical potentials are very similar. This shows that the dynamics does not change significantly from the very low excitation up to the situation with $P = 22$. This situation is unlike the cases of HCP, DCP, HOCl and HOBr[13,14] where the dynamics is quite dependent on the excitation energy or the polyad number.

As mentioned previously, the fixed points are easily identified. They lie on the very top and bottom of the dynamical potentials and they are stable, as shown in Fig.1. In fact, we see that the dynamical potential is characterized by these fixed points.

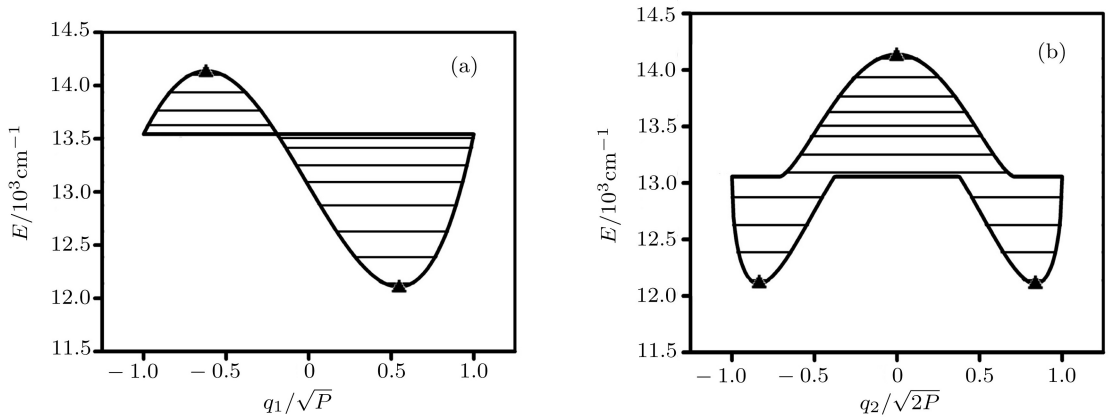


Fig. 1. The dynamical potentials in q_1 (a) and q_2 (b) coordinates, respectively. The state energies are with respect to the zero point energy which is 2366.8 cm^{-1} above the potential well bottom. The stable fixed points, as shown by ▲, are on the top and bottom of the dynamical potentials. See text for details.

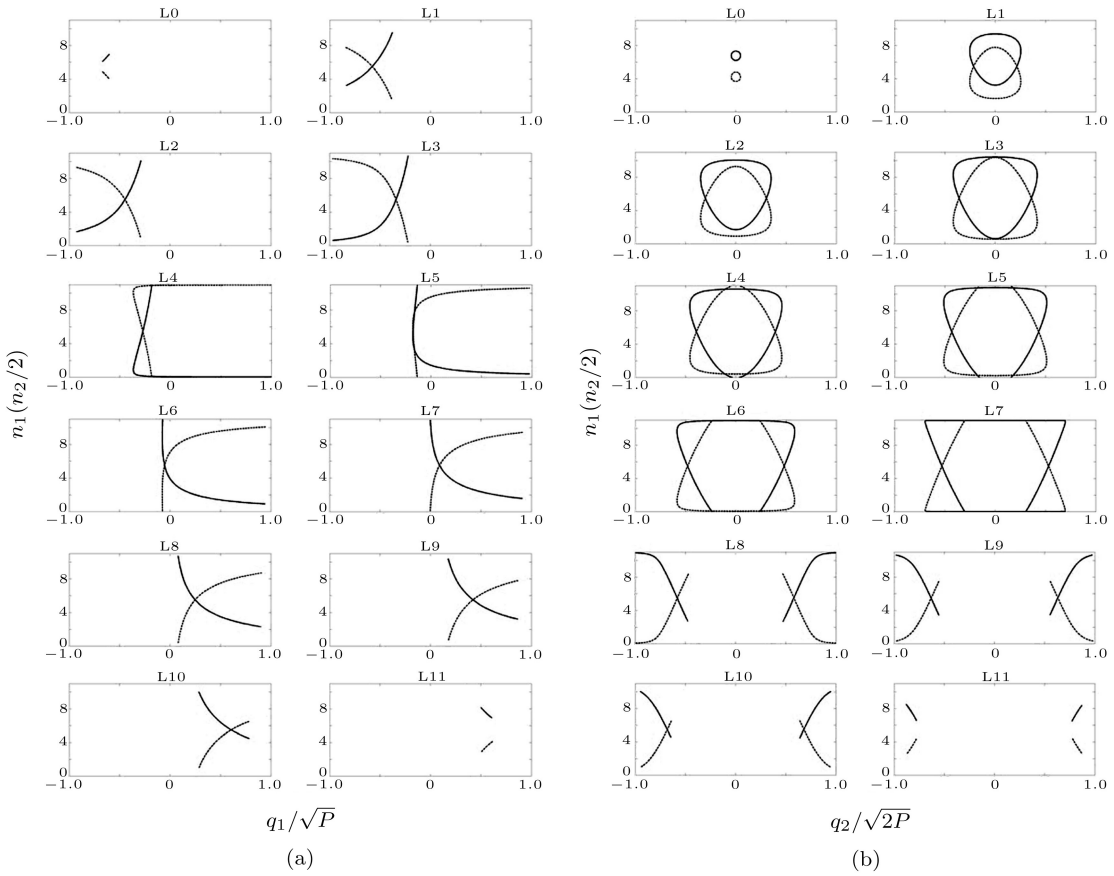


Fig. 2. The action populations of (n_1, q_1)(broken line) and $(n_2/2, q_1)$(solid line). (b) The action populations of (n_1, q_2)(broken line) and $(n_2/2, q_2)$(solid line). See text for details.

The (q_i, p_i) contours for each level can be easily calculated and from which the action populations, (n_1, q_i) and $(n_2/2, q_i)$ can be readily obtained as shown in Figs. 2(a) and 2(b). It is noticeable that except the highest and lowest levels, the curves of (n_1, q_i) and $(n_2/2, q_i)$ intersect somewhere. The implication is that the exchange of actions (energies) on the symmetric stretching and the bending coordinates is significant. This IVR (intramolecular vibrational relaxation) will forbid the action (energy) localization. For the highest and lowest levels, we note that the action on the bending coordinate is always larger than that on the symmetric stretching coordinate. Of course, quantum mechanically, the tunneling effect may enhance IVR in these two levels. This possibility may be greatly reduced for this high excitation with quantum number up to 22. Hence, action localization is highly possible for these two levels. However, as will be shown below, only the lowest level is the real localized mode against the energy excitation.

Figure 3 are the action percentages for the 12 levels sharing $P = 22$. It is noted that the bending motion contributes more to the level dynamics, in general, except for those mid-levels where IVR is also the strongest as can be expected from the action population plots as shown in Figs. 2(a) and 2(b).

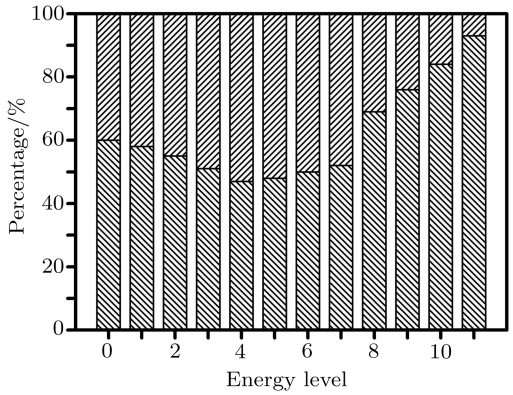


Fig. 3. The action percentages for the 12 levels corresponding to $P = 22$. The lower shadow is for the bending coordinate and the upper shadow is for the symmetric stretching coordinate. The levels are numbered from the highest to the lowest as L0 to L11. See text for details.

Figure 4 shows the action percentages for the lowest level, the lowest level in the upper inverse-Morse well in the q_2 coordinate, (this level is close to the medium one among the levels corresponding to a given polyad number) and the highest level for various polyad number ranging from 12 to 22. It is clearly seen that the dynamical components of the symmetric stretching and bending coordinates for the the lowest level in the upper inverse-Morse well is not robust against the polyad number or energy excitation. As the polyad number increases, its action percentage of the bending coordinate decreases. Strong IVR is the main cause. For the highest level, though its dynamical component of the bending coordinate is significant and its IVR is also not so strong, like the lowest level, as evidenced previously from its action population analysis, its action percentages (of the bending and symmetric stretching coordinates) are not so robust against the polyad number or energy excitation, just like the lowest level in the upper inverse-Morse well. In this sense, we cannot categorize it as a localized level/mode. Instead, the lowest level, whose bending component can be up to more than 90%, stays persistently against the polyad number ranging from 12 to 22. So, it is a real localized bending mode. In fact, we have met with this situation in the cases of HCP, DCP, HOCl and HOBr. We note that in these cases of action localization, there is a common character evidenced in the dynamical potential. The criterion for the appearance of the localized mode is that it is born in the level which possesses an interval centred around nonzero q_i just above a stable fixed point in the dynamical potential. This is indeed a very convenient way for the prediction of the levels that possess action localization and is confirmed again in this nitrous oxide case.

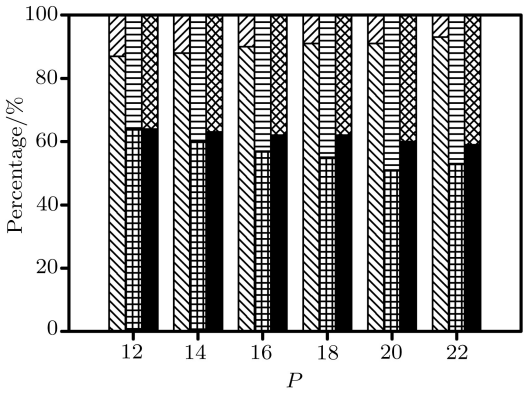


Fig. 4. The action percentages for the lowest level (the left column) , the lowest level in the upper inverse-Morse well in the q_2 coordinate (the middle column) and the highest level (the right column) for the various polyad number P ranging from 12 to 22. The lower shadow is the action percentage of the bending coordinate and the upper shadow is that of the symmetric stretching coordinate. See text for details.

Table 2 shows the action integrals for the levels corresponding to $P = 22$, calculated from (q_1, p_1) and

(q_2, p_2). From the action integrals calculated from (q_1, p_1), the levels can be grouped into two subsets: L0 to L3 and L4 to L11. For the former ones, the action integral increases almost with a constant as the level goes down corresponding to the inverse-Morse well they stay. For the latter ones, the action integral decreases (also almost with a constant) as the level goes down corresponding to the stayed Morse well.

Table 2. The action integrals for the levels corresponding to $P = 22$.

state label	action integral in (q_1, p_1) space	difference between neighbouring levels	action integral in (q_2, p_2) space	difference between neighbouring levels
L0	0.03	/	0.07	/
L1	1.02	0.99	2.01	1.94
L2	2.00	0.98	4.03	2.02
L3	2.95	0.95	5.91	1.88
L4	7.19	/	7.59	1.68
L5	6.18	−1.01	9.62	2.03
L6	5.13	−1.05	11.69	2.07
L7	4.12	−1.01	13.73	2.04
L8	3.11	−1.01	6.23	/
L9	2.10	−1.01	4.21	−2.02
L10	1.08	−1.02	2.19	−2.02
L11	0.08	−1.00	0.17	−2.02

From the action integrals calculated from (q_2, p_2), the levels can be grouped into two subsets, also with constant increment (decrement) in their action integrals: L0 to L7 and L8 to L11. For the former ones, the action integral increases as the level goes down corresponding to the inverse-Morse well stayed with minor deviation on L4. For the latter ones, the action integral decreases as the level goes down corresponding to the stayed Morse wells. The constant action integral increment/decrement demonstrates the compatibility of our classical treatment with the quantized levels. These classifications also show that the levels, though belonging to the same polyad number, stay in various dynamical environments which are defined essentially by the classical fixed points.

5. Concluding remarks

The highly excited vibrational dynamics of nitrous oxide is studied with anharmonicity and Fermi coupling between the symmetric stretching and bending coordinates via the dynamical potentials and the related algorithms. The merit of this approach is that it does not count on the details of each level (though it does count on, to a certain extent) through the solution of the wave functions. Instead, this approach views the dynamics from a global sense that the vibrational dynamics of various systems such as HCP, DCP, HOCl, HOBr and nitrous oxide can be compared on a common footing. The results are impressing that though these systems are different, they share much dynamical similarity. The merit is that the classical dynamical variables, especially the fixed points, play the essential dynamical roles even for a quantum system.

Of course, the adopted algebraic Hamiltonian is a simplified one without the coupling with the antisymmetric stretching coordinate. The inclusion of this coupling is inevitable during the whole dynamical process which will lead to a chaotic motion. However, the dynamical study with this adopted Hamiltonian is still of value since by this way, we can understand some important facets of the complicated dynamical behaviour of the molecule as a whole which, otherwise, would be very hard to grasp once for all. Finally, the application of this dynamical potential approach to non-integrable systems could be interesting and needs elaboration as we have done in our works on DCO[10] and HCO.[11]

References

[1] Teffo J L, Perevalov V I and Lyulin O M 1994 *J. Mol. Spectrosc.* **168** 390
[2] Champargue A, Permogorov D, Bach M, Temsamani M A, Auwera J V, Herman M and Fujii M 1995 *J. Chem. Phys.* **103** 5931
[3] Waalkens H, Jung C and Taylor H S 2002 *J. Phys. Chem.* A **106** 911
[4] Arnold V I 1978 *Mathematical Methods of Classical Mechanics: Graduate Texts in Mathematics* Vol.**60** (Berlin: Springer)
[5] Lu Z M and Kellman M E 1997 *J. Chem. Phys.* **107** 1
[6] Xiao L and Kellman M E 1989 *J. Chem. Phys.* **90** 6086
[7] Kellman M E 1990 *J. Chem. Phys.* **93** 6630
[8] Jung C and Taylor H S 2007 *J. Phys. Chem.* A **111** 3047
[9] Kellman M E 1985 *J. Chem. Phys.* **83** 3843
[10] Huang J and Wu G Z 2007 *Chem. Phys. Lett.* **439** 231
[11] Fang C and Wu G Z 2009 *Chin. Phys.* B **18** 130
[12] Svitak J, Li Z, Rose J, and Kellman M E 1994 *J. Chem. Phys.* **102** 4340
[13] Fang C and Wu G Z 2009 *J. Mol. Struct.: Theochem.* **910** 141
[14] Fang C and Wu G Z 2010 *Chin. Phys.* B **19** 010509
[15] Heisenberg W 1925 *Z.Physik* **33** 879
[16] Wu G Z 2005 *Nonlinearity and Chaos in Molecular Vibrations* (Amsterdam: Elsevier)